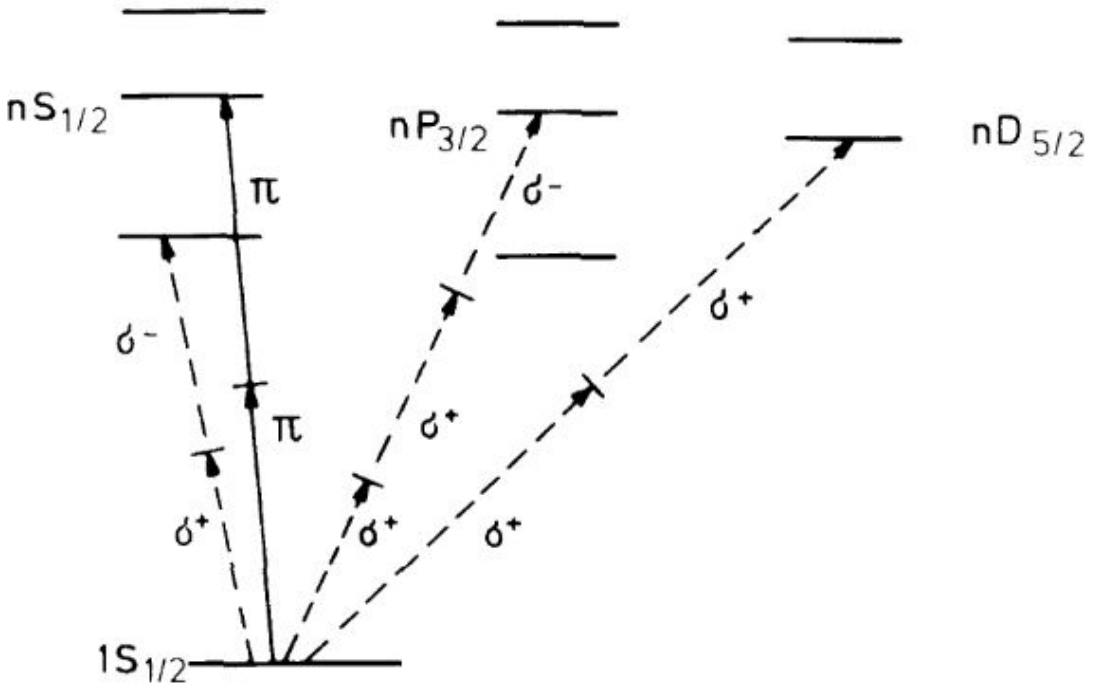

Fig. 7.27. Different two-photon transitions in an atom, depending on the polarization characteristics $\hat{e}_1$ and $\hat{e}_2$ of the two laser fields

ВЕРОЯТНОСТЬ ДВУХФОТОННЫХ ПЕРЕХОДОВ

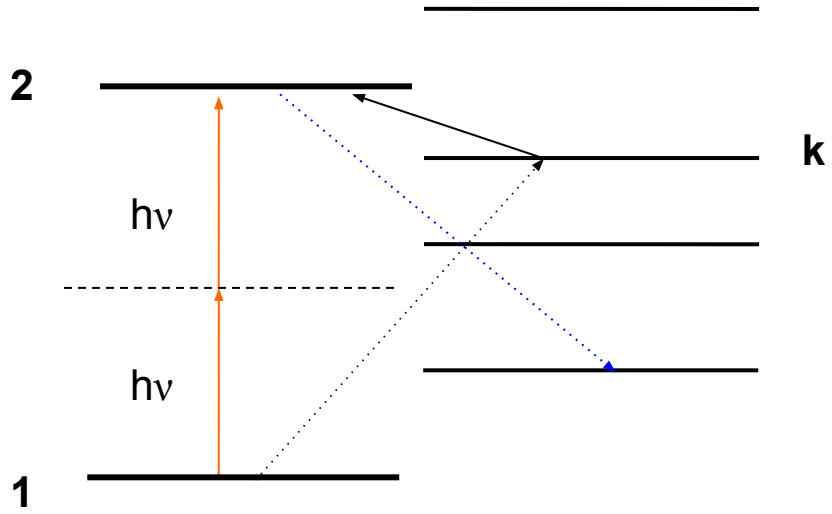

$$A_{12} = \left[\frac{4\gamma_{12}}{(\omega_{12} - 2\omega)^2 + (\gamma_{12}/2)^2} + \frac{\gamma_{12}}{(\omega_{12} - 2\omega - 2kv)^2 + (\gamma_{12}/2)^2} + \frac{\gamma_{12}}{(\omega_{12} - 2\omega + 2kv)^2 + (\gamma_{12}/2)^2} \right] X$$

$$X \left| \sum_k \frac{(\vec{d}_{1k}\vec{e}_1)(\vec{d}_{k2}\vec{e}_2)}{(\omega - \omega_{1k})} + \sum_k \frac{(\vec{d}_{1k}\vec{e}_2)(\vec{d}_{k2}\vec{e}_1)}{(\omega - \omega_{1k})} + \right|^2$$

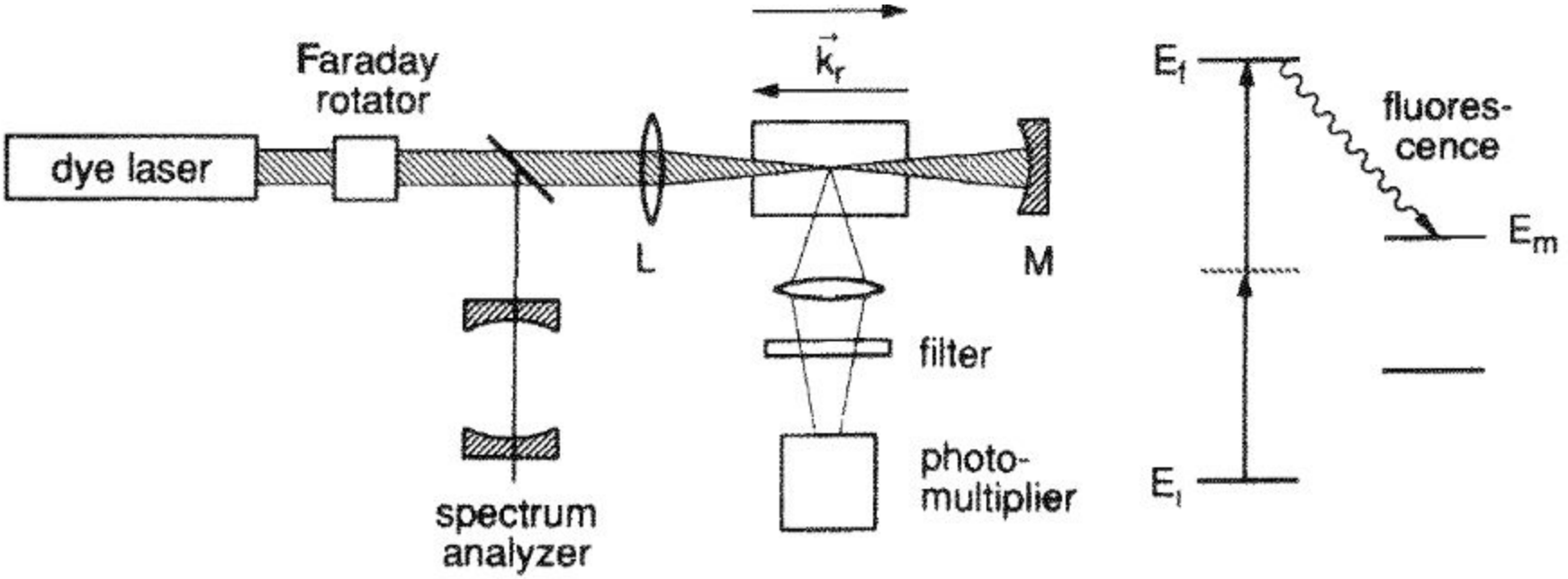

Fig. 7.28. Experimental arrangement for Doppler-free two-photon spectroscopy

ДВУХФОТОННАЯ СПЕКТРОСКОПИЯ

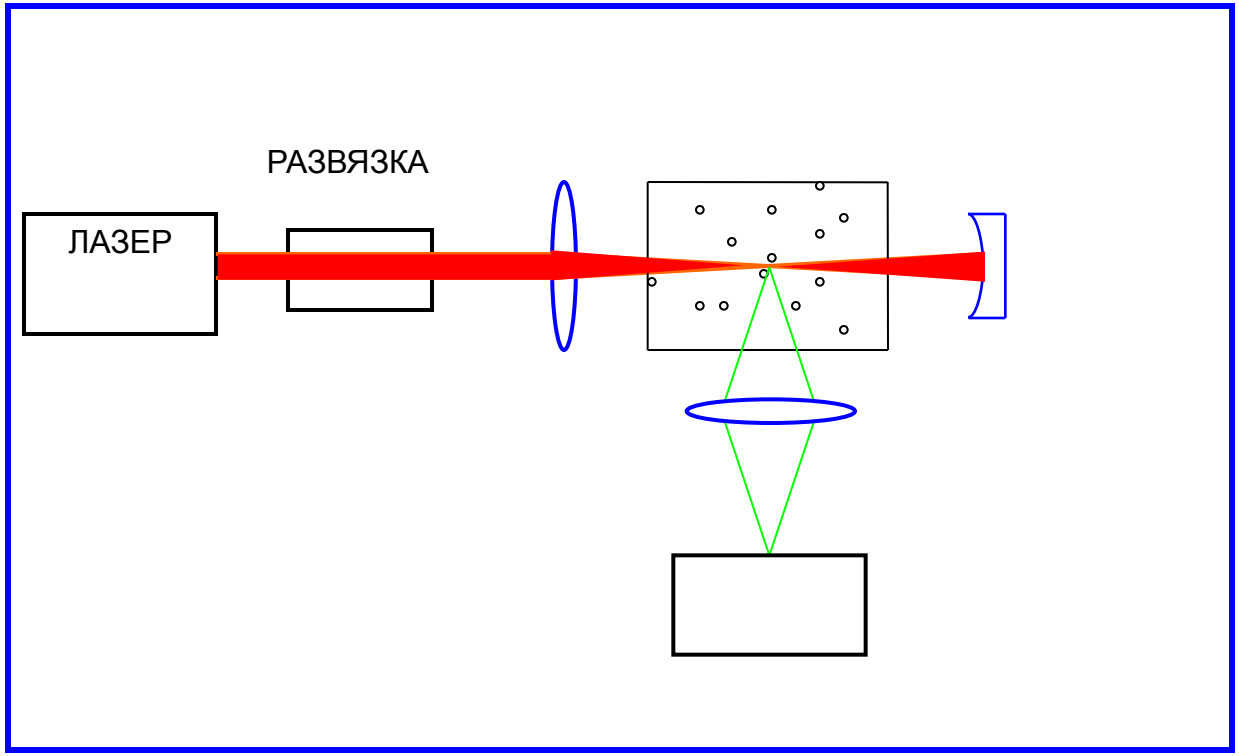

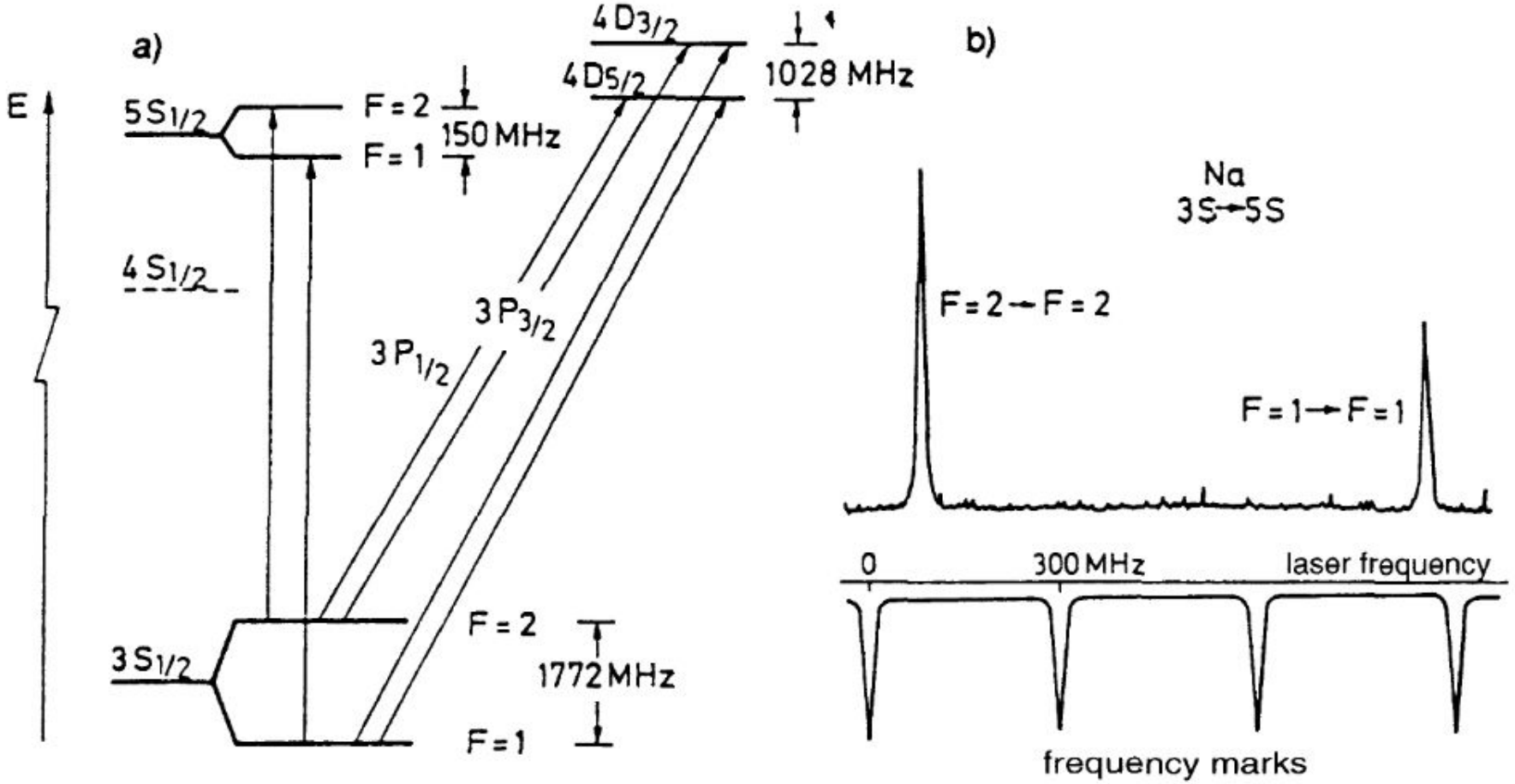

Fig. 7.29a,b. Doppler-free two-photon spectrum of the 3S → 5S and 3S → 4D transitions in the Na atom: (**a**) level scheme; (**b**) 3S → 5S transition with resolved hyperfine structure [7.43]

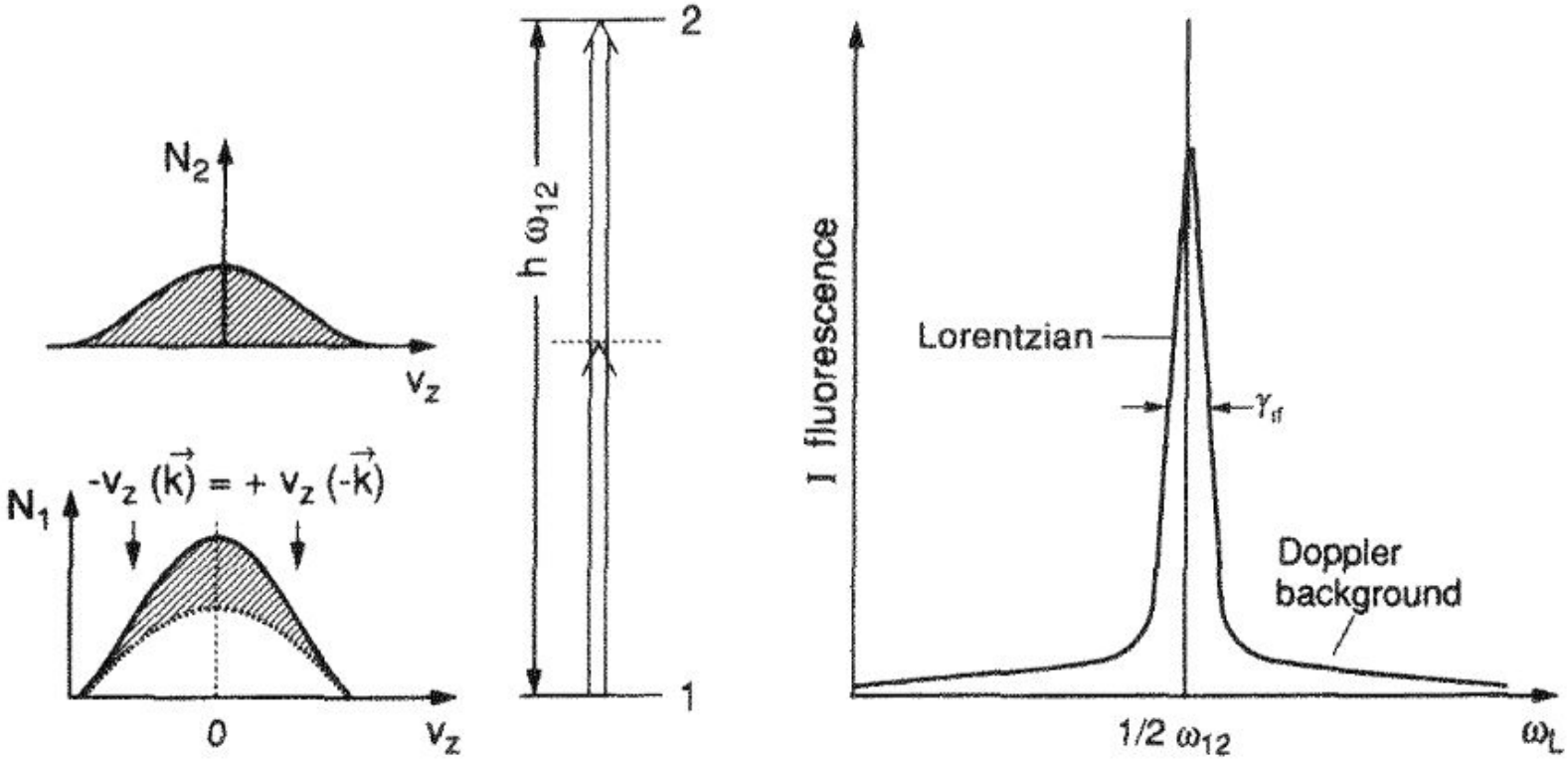

Fig. 7.30. Schematic line profile of a Doppler-free two-photon signal with (greatly exaggerated) Doppler-broadened background

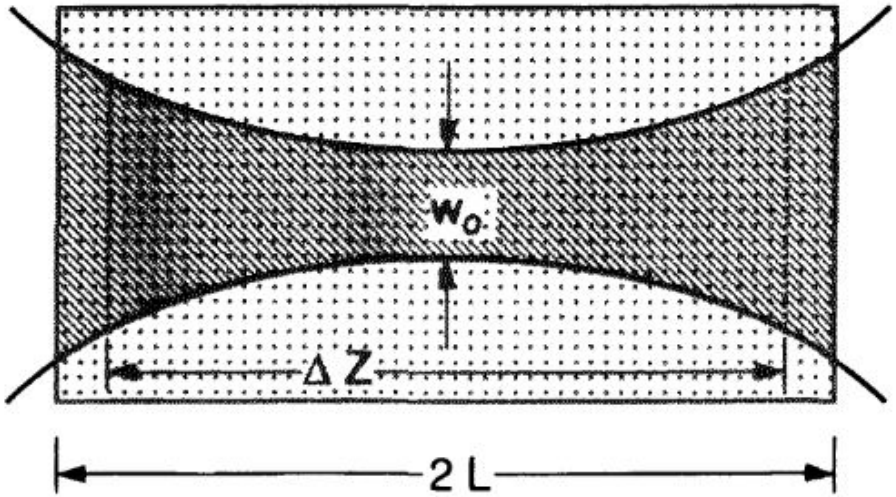

Fig. 7.31. Beam waist w_0 and Rayleigh length L for optimum focusing in two-photon spectroscopy

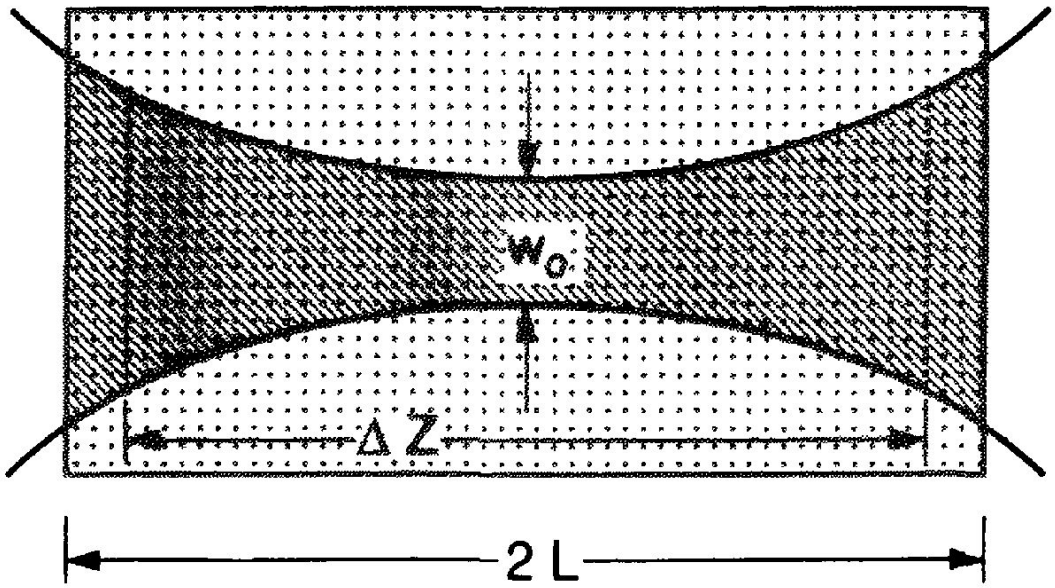

$$L = \pi w_0^2/\lambda$$

$$\int_z \int_r I^2(r, z) 2\pi r \, dr \, dz \,, \qquad I(r, z) = \frac{2P_0}{\pi w^2} e^{2r^2/w^2}$$

$$w(z) = w_0 \sqrt{1 + \frac{\lambda z}{\pi \gamma w_0^2}} \,, \qquad w_0 = (\lambda R/2\pi)^{1/2} \,.$$

$$\int_{-\Delta z/2}^{+\Delta z/2} \frac{\mathrm{d}z}{1+\left(\lambda z/\pi w_0^2\right)^2} = 2L \arctan[\Delta z/(2L)] \,,$$

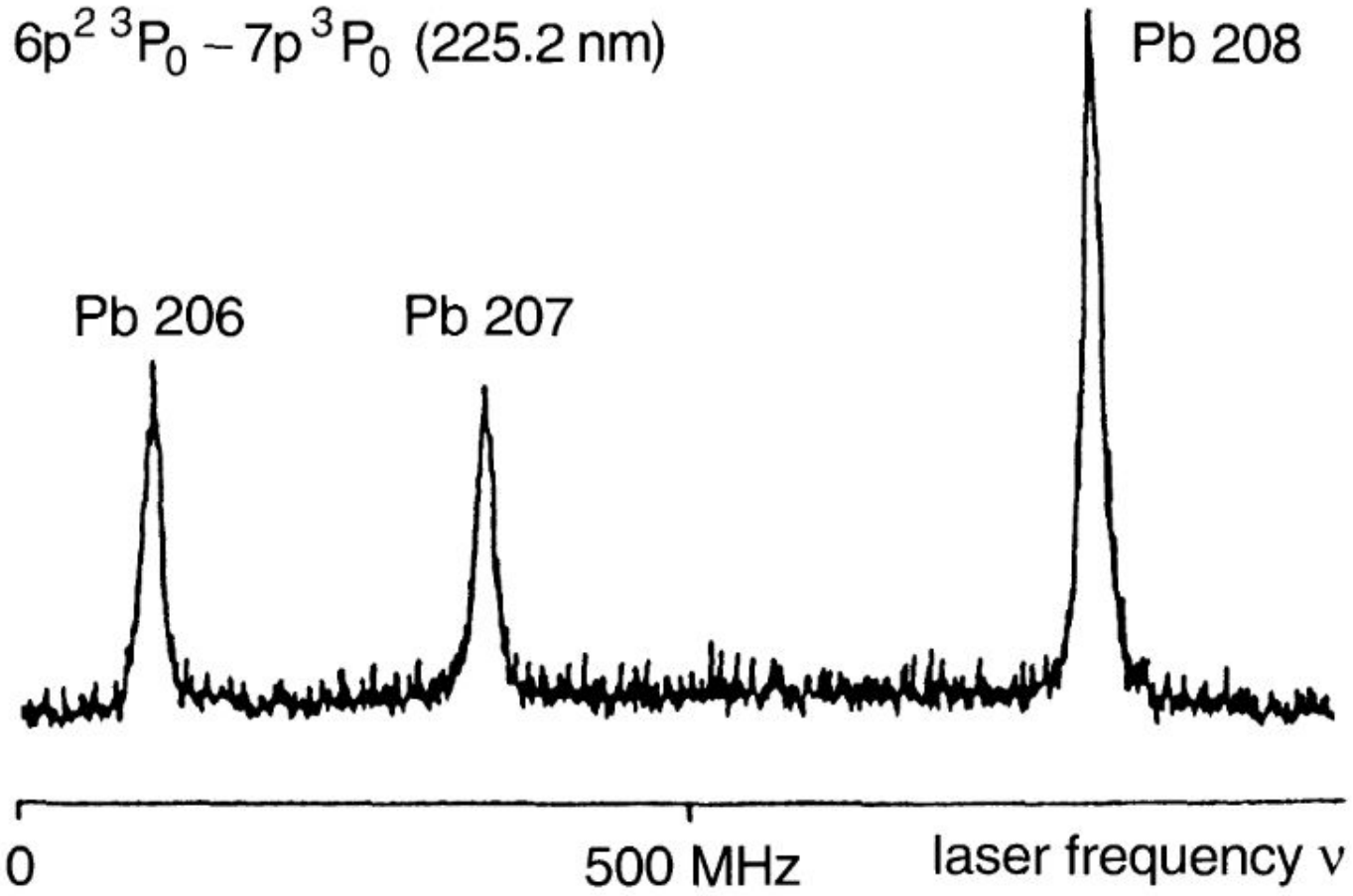

Fig. 7.32. Measurement of the isotope shift of the stable lead isotopes measured with Doppler-free two-photon spectroscopy at $\lambda_{exc} = 450\,nm$ and monitored via fluorescence [7.48]

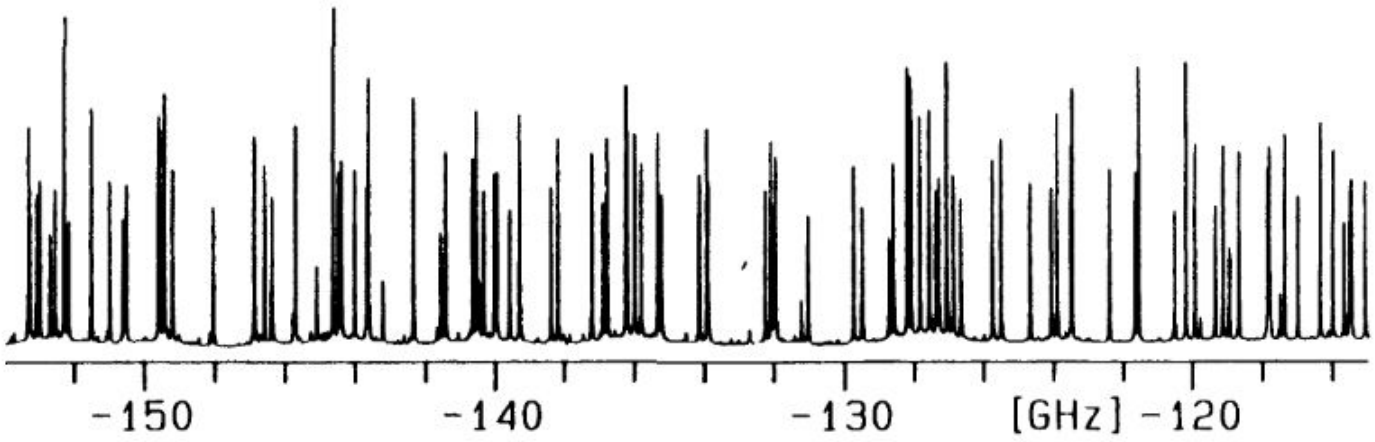

Fig. 7.33. Section of the Doppler-free two-photon excitation spectrum of the 14_0^1 Q_Q band of C_6H_6 [7.53]

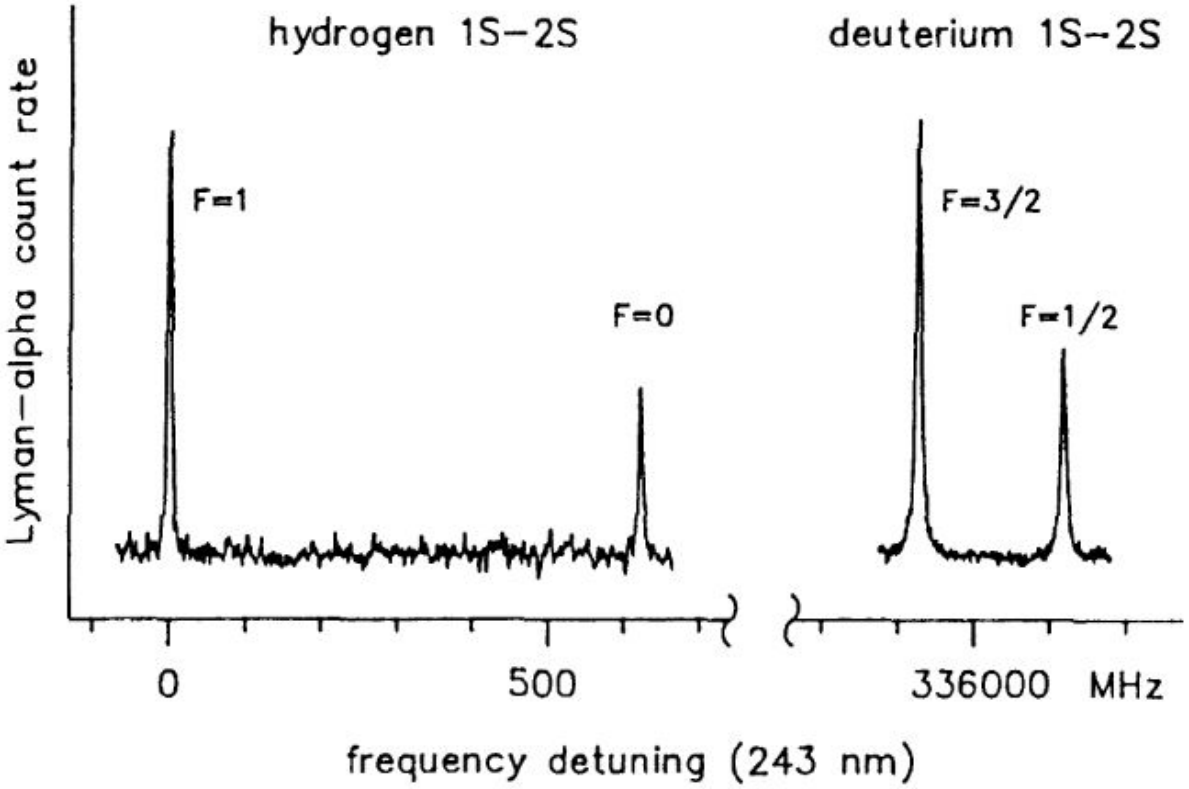

Fig. 7.34. Doppler-free two-photon transitions of hydrogen $1S-2S$ and deuterium $1S-2S$ [7.58]